Aceh Int. J. Sci. Technol., 11(1): 85-96
April, 2022
doi: 10.13170/aijst.11.1.24181

Aceh International Journal of Science and Technology
ISSN: p-2088-9860; e-2503-2398
Journal homepage: http://jurnal.unsyiah.ac.id/aijst

Construction of Hierarchical $CuCo_2O_4$-$Ni(OH)_2$ Core-Shell Nanowire Arrays for High-Performance Pseudocapacitors

Ilham Azmy[1,*], Jun Wang[2]

[1]Department of Mechanical Engineering, Bandung State of Polytechnic, Bandung, Indonesia
[2]College of Materials Science and Chemical Engineering, Harbin Engineering University, Harbin, PR China
*Corresponding author email: ilham.azmy@polban.ac.id

Received : April 1, 2022
Accepted : April 27, 2022
Online : April 30, 2022

Abstract – The hierarchical $CuCo_2O_4$-$Ni(OH)_2$ core-shell nanowire arrays on Ni foam were fabricated using facile and cost-effective two-step hydrothermal synthesis. The growth of $CuCo_2O_4$ nanowires was developed on Ni foam as the apposite basis of the conductive scaffold, and the ultrathin $Ni(OH)_2$ nanowires were subsequently immobilized to form $CuCo_2O_4$-$Ni(OH)_2$ core-shell nanowire arrays (NWAs). The prepared materials were further characterized in structural, morphological, and electrochemical properties. The obtained CuCo2O4-$Ni(OH)_2$ pseudocapacitor electrode, incorporated by unique core-shell heterostructures nanowire arrays, exhibited great specific capacitance of 1201.67 F g^{-1} at 1 mA g^{-1}, which is much higher than pristine $CuCo_2O_4$ nanowire of 638.89 F g^{-1} at 1 mA g^{-1}. Simultaneously, it also has a high power density of 5.56 kW kg^{-1} at an energy density of 73.33 Wh kg^{-1} and good long-term cycling performance (~84 capacitance retention after 1000 cycles). The improved morphological and structural properties have substantiated the $CuCo_2O_4$-$Ni(OH)_2$ core-shell nanowire arrays properties owing to higher surface active area and richer redox activity for boosting the electrochemical properties.

Keywords: $CuCo_2O_4$, $Ni(OH)_2$, Core-shell structure, Supercapacitors, Nanosheet arrays.

Introduction

The depletion of fossil fuels and other energy resources has been contemporaneously changing human minds to utilize energy in safe ways. By now, with also mentioning apprehensive climate change, it is crucial to find clean and reliable energy to save the world's sustainability. Energy storage technology (viz., batteries, fuel cells, and supercapacitors) is a fundamental property in the effort to harvest clean and sustainable energy (Yu et al., 2015). In the era of advanced technology, recent developments in energy storage technology have led to a renowned interest in supercapacitors (SCs), which have emerged as a powerful devices compared to batteries. SCs, also known as electrochemical capacitors, have been used in a wide area of energy harvesting and storage applications such as portable electronics and grid power instruments (Dyatkin et al., 2013). SCs can be classified into electrical double layer capacitors (EDLC) and pseudocapacitors according to the charge storage mechanism. Pseudocapacitors shows promising characteristics to achieve battery-level energy density, which concomitances with the high power density and long cycling stability due to reversible fast redox (faradaic) reactions occurring at the surface of the electrode in term of charge storage properties (V. C. Lokhande, Lokhande, Lokhande, Kim, & Ji, 2016). Referring to these unique characteristics, researchers have pointed out their consideration of achieving high-performance supercapacitors by the pseudocapacitance mechanism.

The critical part of supercapacitors is electrode material, which garnered electrical energy during charge-discharge processes. It is widely believed that electrode materials are firmly decisive in developing high-

performance supercapacitors. Metal oxides comprise unique chemical and physical properties and have become genuine emphasis as electrode material candidates for supercapacitors. A big chance of metal oxides utilization could be associated with its large electrochemical performance, wherein it also stores energy similar to batteries that enable high energy density ascribed from ultrafast surface redox reaction(C. D. Lokhande, Dubal, & Joo, 2011; Wu et al., 2012; Xu et al., 2014). Furthermore, SCs based metal oxide materials have been augured to bridge the gap with batteries, thus improving their energy density affirmed with cycle life and power density.

In recent times, ternary transition metal oxide, particularly spinel cobaltite materials ACO_2O_4 (A=divalent metal cations), has attracted researchers due to their multiple oxide states, environmental benignity, high theoretical capacitance, and applicable expenses as electrode materials for supercapacitors 10. Several attempts have been devoted to fabricating spinel cobaltite materials such as $NiCo_2O_4$, $CuCo_2O_4$, $MgCo_2O_4$, $ZnCo_2O_4$, $MnCo_2O_4$, and $FeCo_2O_4$(Chen et al., 2013; Cui et al., 2016; Khalid et al., 2015). In the midst of these materials, $CuCo_2O_4$ has been investigated as a promising candidate for SCs electrodes due to its abundant electrochemical activity, strong chemical stability, eco-friendly, and inexpensive. Additionally, $CuCo_2O_4$ has significantly ameliorated electrochemical and physiochemical characteristics by the fusion of Cu^{2+} to Co^{2+} compared with Co_3O_4(Shude Liu, San Hui, Hui, Yun, & Kim, 2016; Pendashteh et al., 2015). $CuCo_2O_4$ also exhibits high capacitive performance and reaction kinetics than single component copper oxides (CuO) and cobalt oxide (Co_3O_4).

Moreover, it remains inhibitions such as the capacitance and operation voltage task to improve $CuCo_2O_4$-based electrodes to obtain high-performance supercapacitors. One of the key strategies for successful breakthroughs is to construct desirable core-shell structure materials. The unique core-shell structure possesses numerous advantages in improving the electrochemical performance of supercapacitors. It is not only availed to enhance active surface area and short ions diffusion pathways but also bestows fully synergistic effects toward each component. Arising from this phenomenon, many researchers attempted to manufacture SCs materials based on core-shell structures.

Nickel hydroxides, $Ni(OH)_2$, has vastly studied and recognized as attractive transition hydroxides materials for supercapacitors. $Ni(OH)_2$ shows remarkable properties with regard to ultrahigh theoretical capacitance, well-defined electrochemical redox activity, environmentally benign, and low-price(Chuo et al., 2014; Kurra, Alhebshi, & Alshareef, 2015; L. Zhang et al., 2016). However, lower power density, poor cycling stability, and rate capability resulted from poor electrical conductivity because of the indisposed wrinkling and bulging during the charge-discharge process. To chase the requisite of increased capacitance and superior rate capability performance during the fast charge-discharge process, a smart approach and well-design configuration of innovative hybrid materials has tied momentous attention owing to excellent electrochemical performance through synergistic effects among each component, respectively. Therefore, an expected design can be attempted to construct $CuCo_2O_4$-$Ni(OH)_2$ core-shell nanostructures for supercapacitors. Several strategies have been developed to fabricate ternary metal oxide combined with $Ni(OH)_2$ hybrid structure. For instance, Li et al.(W. Li et al. 2015) described the temperature effects of pseudocapacitance performance $NiCo_2O_4$@$Ni(OH)_2$ with high electrochemical performance by virtue of this aforementioned composite electrode. Zhao et al.(Y. Zhao, Hu, Zhao, & Wu, 2016) demonstrated the fabrication of multicomponent $MnCo_2O_4$@$Ni(OH)_2$ belt-based core-shell nanoflowers with significantly enhanced specific capacitance, high energy density, and long cycling lifespan as anode material. Pan et al.(Pan et al., 2017) reported the hierarchical $ZnCo_2O_4$@$Ni(OH)_2$ nanosheets composite structures with improved ultrahigh areal capacitance, high energy density, and excellent rate capability. Some investigations said seem to suggest a pertinent role for hybrid structure transition metal oxide/hydroxides. These strategies have illustrated that $CuCo_2O_4$ and $Ni(OH)_2$ have distinct possibilities to become hybrid core-shell nanostructures materials that further acquire good electrochemical properties.

We have first fabricated $CuCo_2O_4$ nanowires@$Ni(OH)_2$ core-shell nanowire arrays grown on Ni foam via a facile two-step hydrothermal process. The combined structures among both materials have improved electrochemical behaviors of high specific capacitance of 1201.67 F g^{-1} at 1 mA g^{-1}. The enhanced power density of 5.56 kW kg^{-1} at an energy density of 73.33 Wh kg^{-1} and good long-term cycling performance.

Materials and Methods

Nickel foam was directly used as a conductive substrate, with a thickness of 1 mm, and 98% porosity. All chemical reagents and materials in this work were used of analytical grade without further purification.

Treatment of Ni foam

Ni foam was directly used as a conductive substrate in this experiment. Ni foam (4 x 2 cm^2) was ultrasonicated in 3M diluted HCl to remove the NiO layer on the surface. Treated Ni foam was cleaned successively with DI water and absolute ethanol several times, followed by drying at 25 ^{0}C overnight.

Synthesis of $CuCo_2O_4$ nanowire on Ni Foam

In a typical synthetic process, 1 mmol of $Cu(NO_3)_2.3H_2O$, 2 mmol of $Co(NO_3)_2.6H_2O$, and 5 mmol of $CO(NH_2)_2$ were dissolved in 35 mL DI water under continual magnetic stirring to form a uniform light blush solution. After that, a piece of Ni foam and the as-prepared solution was carefully transferred into a 50 mL Teflon-Lined stainless-steel autoclave and reacted under 120 ^{o}C for 6 h. By naturally cooling the autoclave to ambient temperature, the as-prepared samples were washed by ethanol and DI water successfully dried at 60 ^{o}C for 10 h. Finally, the samples were annealed at 300 ^{o}C for 3 h to obtain $CuCo_2O_4$ nanowires yield on Ni foam.

Preparation of hierarchical $CuCo_2O_4$-$Ni(OH)_2$ core-shell heterostructures nanowire arrays (NWs) on Ni Foam

The facile hydrothermal method prepared the synthesis process of Ni(OH)2 nanosheets onto CuCo2O4 nanowires/Ni foam surface. In a typical procedure, 3 mmol of $Ni(NO_3).6H_2O$ and 6 mmol of $CO(NH_2)_2$ were dissolved in 35 mL DI water while stirred until form a light verdant solution. A piece of Ni foam covered with $CuCo_2O_4$ and the solution were then placed into a Teflon-lined stainless steel autoclave and gradually heated up to 100 ^{o}C for 6 h. was washed with ethanol and DI water at 60 ^{o}C for 10 h.

Materials Characterization

The crystal and phase structure of the synthesized materials was characterized by X-Ray Diffraction (XRD, Philips X'Pert Pro) equipped with Cu Kα radiation (λ = 0.15406 nm) in the 2θ range of 20^o-80^o. The morphological structures of the samples were investigated by Scanning Electron Microscopy (SEM, Zeiss, Gemini-500) and Transmission Electron Microscopy (TEM, JEOL, JEM-2100) with a field of emission gun operated at 200 kV. The chemical composition of materials was measured by X-Ray Photoelectron Spectroscopy (XPS; PHI5700 ESCA spectrometer with Al Kα radiation, hv=1486.6 eV). The surface area and porosity of materials were determined by nitrogen adsorption-desorption isotherm at the boiling point of nitrogen temperature (77 K) using a Micromeritics ASAP 2010 surface area and pore size distribution analyzer instruments.

Electrochemical Measurements

The electrochemical measurements of prepared materials $CuCo_2O_4$ NW and $CuCo_2O_4$-$Ni(OH)_2$ NWAs were evaluated in an electrochemical workstation CHI760i (Shanghai Chenhua Instruments Ltd., China) via a traditional three-electrode system. The prepared materials were used as working electrodes (1 x 1 cm^2), and platinum electrodes and Ag/AgCl electrodes were used as reference electrodes and counter electrodes. The mass loading of materials ($CuCo_2O_4$ ≈ 1.8 mg and $CuCo_2O_4$-$Ni(OH)_2$ ≈ 2.4 mg) on Ni foam substrate were tested for all electrochemical tests. Cyclic voltammetry (CV), galvanostatic charge-discharge (GCD), and electrochemical impedance spectroscopy (EIS) tests were evaluated in 3M KOH aqueous electrolyte at room temperature. CV test was carried out in a potential range between -0.1 V to 0.6 V at a varying scan rate of 2, 5, 8, 10, and 20 mV s^{-1}. Galvanostatic charge-discharge measurement was conducted between 0 to 0.5 V with current densities ranging from 1, 5, 10, 20, and 40 mA g^{-1}. EIS was conducted using an amplitude of 5 mV in the frequency range from 0.01 Hz to 100 kHz. The specific capacitance was calculated by using the Equation:

$$Cm = \frac{I\,x\,t}{m\,x\,\Delta V} \quad (1)$$

Where Cm (F g^{-1}) is the specific capacitance, I (A) is the discharge current density, t (s) is the discharge time, m (g) is the active material mass on the electrode, and ΔV (V) is voltage alteration. The energy density was calculated by using the formula:

$$E = \frac{1}{2}\ Cm\,x\,\Delta V^2 \quad (2)$$

Where E is energy density (Wh kg^{-1}), Cm is the obtained specific capacitances (F g^{-1}), and ΔV (V) is voltage change.

$$P = \frac{E}{t} \quad (3)$$

Where P is power density (kW kg^{-1}), E is the obtained energy density (Wh kg^{-1}), and t is the discharged time (s).

Results

Structural and Morphological Characteristics

In this study, a novel strategy has been exerted to synthesize hierarchical $CuCo_2O_4$-$Ni(OH)_2$ core-shell nanowire arrays (NWs) on 3D Ni foam as conductive substrate via facile two steps hydrothermal method. Core-shell nanostructures arrays on 3D Ni foam are alluring according to the synergistic effect between its rational design and unique structure. The facile strategy of $CuCo_2O_4$-$Ni(OH)_2$ core-shell NWs on Ni foam is schematically illustrated in **Figure 1**.

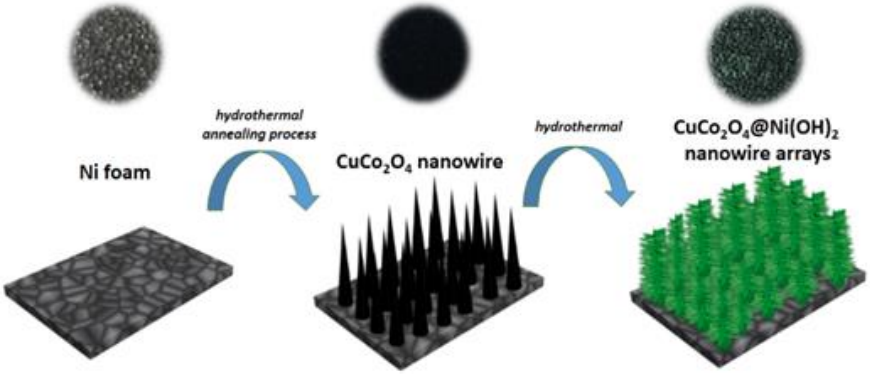

Figure 1. Schematic illustration of formation process hierarchical $CuCo_2O_4$-$Ni(OH)_2$ core-shell heterostructures nanowire arrays grown on Ni foam.

At the beginning process, $CuCo_2O_4$ grew up and formed as Cu-Co hydroxides precursor due to urea's slow hydrolysis and in situ release of OH and CO_3^{2-} in hydrothermal reaction(Cheng et al., 2015; S. Liu, Hui, & Hui, 2016). This process also initiated the precipitation of Cu^{2+} and Co^{2+} that started the nucleation period of $CuCo_2O_4$ on Ni foam. $CuCo_2O_4$ nanowire was obtained after annealing treatment. The relevant reaction of the series process can be followed in this Equation (Anu Prathap, Wei, Sun, & Xu, 2015; Hu et al., 2015):

$$2\ CO(NH_2)_2 + 5\ H_2O \rightarrow 4\ NH^{4+} + 2\ OH^- + CO_3^{2-} + CO_2 \quad (4)$$
$$(Co^{2+}, Cu^{2+}) + CO_3^{2-} + 2\ OH^- \rightarrow (Co, Cu)_2(CO_3)(OH)_2 \quad (5)$$
$$Cu_2(CO_3)(OH)_2 + 2\ Co_2(CO_3)(OH)_2 + O_2 \rightarrow 2\ CuCo_2O_4 + 3\ CO_2 + 3\ H_2O \quad (6)$$

The assemblage of ultrathin $Ni(OH)_2$ nanowire arrays was easily deposited onto Ni foam@$CuCo_2O_4$ nanowire via a second hydrothermal reaction by using nickel nitrate and urea as the precursor solution. Urea was used as a hydrolysis agent to release OH− ions due to its easy decomposition rate and relatively react in mild pH conditions. The decomposition of urea transpired by Ni^{2+} and OH^- an initial reaction which then stimulates $Ni(OH)_2$ nucleation and rapidly thrives into prime particles, thus can be responded to following reaction equation:

$$NO_3^- + H_2O + 2\ e^- \rightarrow NO_2^- + 2\ OH^- \quad (7)$$
$$Ni^{2+} + 2\ OH^- \rightarrow Ni(OH)_2 \quad (8)$$

Henceforth, $Ni(OH)_2$ nuclei grew up to be primary particles step by step. These primary particles accumulated into chains, thus slightly amassed on the surface of Ni foam@$CuCo_2O_4$ nanowire to become the aggregation cores of more amorphous primary particles. As the $Ni(OH)_2$ particles continue to aggregate, $Ni(OH)_2$ begins to crystallize and grow along the c-axis, gradually forming nanowire arrays (NWs) and eventually constructing the $CuCo_2O_4$-$Ni(OH)_2$ core-shell nanowire arrays (NWs).

The X-Ray Diffraction (XRD) measurements were tested to analyze the phase and crystallite structure of materials. The materials were scraped from Ni foam to obtain powder samples. **Figure 2a** shows XRD patterns of $CuCo_2O_4$ and $CuCo_2O_4$-$Ni(OH)_2$ samples. All corresponding peaks of $CuCo_2O_4$, located at 31.1°, 36.7°, 43.4°, 44.6°, 50.7°, 59.5°, 64.9°, 73.8°, 76.5°, can be indexed to the (220), (311), (222), (400), (422), (511), (440), (620) and (533) planes respectively, affirming to the presence of the cubic $CuCo_2O_4$ phase (JCPDS 78-2176). Moreover, $CuCo_2O_4$-$Ni(OH)_2$ diffraction peaks are marked by the existence of derived peaks from the hexagonal $Ni(OH)_2$ phase (JCPDS 73-1520). The clear signal of $Ni(OH)_2$ can be identified from XRD patterns, signing the good crystallinity and adequate amount of the $Ni(OH)_2$.

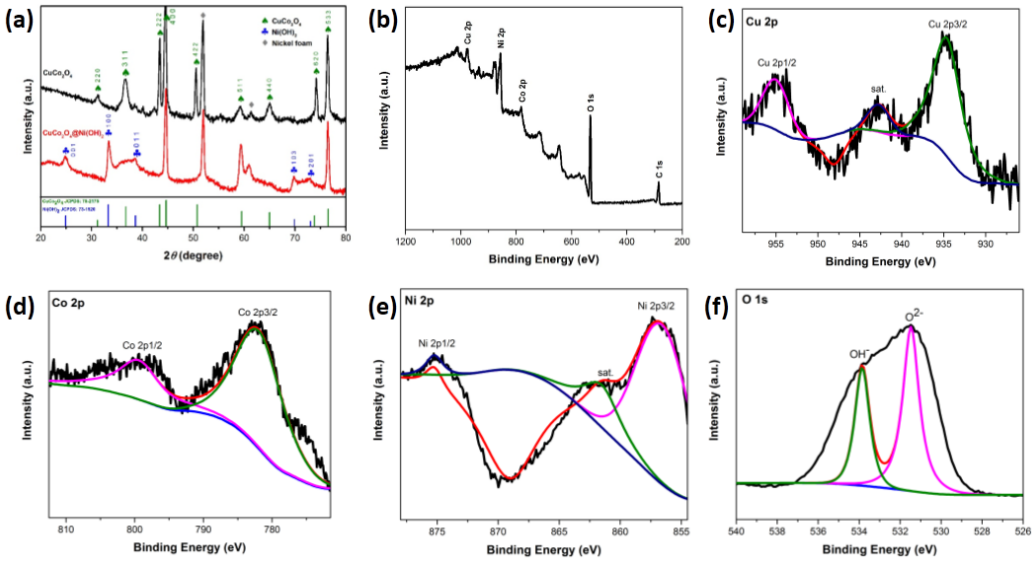

Figure 2. (a) XRD patterns of $CuCo_2O_4$ nanowire and hierarchical $CuCo_2O_4$-$Ni(OH)_2$ core-shell NW scratched from Ni foam. (b) XPS general spectra of hierarchical $CuCo_2O_4$-$Ni(OH)_2$ core-shell heterostructures NWAs scratched from Ni foam; and (c~f) the corresponding XPS survey scans of Cu 2p, Co 2p, Ni 2p, and O 1s, respectively.

The hydrothermal methods are favorable for obtaining pure $Ni(OH)_2$. Apart from significant peaks, the emanation of two peaks at about 52° and 61° are ascribed from Ni foam. Therefore, all diffraction peaks align with XRD standards and firmly demonstrate the efficacious fabrication of $CuCo_2O_4$-$Ni(OH)_2$ on Ni foam.

To get further information about the chemical composition of products, XPS measurement was tested and analyzed by the Gaussian method in the peak fitting process. The overall scan spectrums of $CuCo_2O_4$-$Ni(OH)_2$ can be shown in Figure 2b, presenting the survey scan area of the sample's Cu, Co, Ni, and O elements. As depicted in Figure 2c, the Cu spectra located in the range 954.5 eV and 934.6 eV were assigned to the binding energy of Cu $2p_{1/2}$ and Cu $2p_{3/2}$. Besides, Cu satellite peaks at 942.7 eV and 963.1 eV indicate the spin-orbit characteristic of Cu^{2+}. Figure 2d depicts the apparent spectrum of Co 2p, which is well-marked by the main two peaks revealed at binding energy 798.1 and 781.8 eV ascribed from Co $2p_{1/2}$ and Co $2p_{3/2}$, respectively. More accurately, several resolved peaks located at around 803.3 eV and 786.6 eV correspond to the Co^{2+} state; afterward, another resolved peaks at 798.1 eV and 781.8 eV are assigned to Co^{3+}, ultimately, the final peak at 775.7 eV is attributed to Co^{4+} state. Figure 2e shows the Ni species spectrum at binding energy 874.7 and 856.6 eV, attributed to Ni $2p_{1/2}$ and Ni 2p3/2 of Ni(OH)2. After the fitting peaks processes, it has been founded that the deconvoluted peaks at 874.7 eV and 856.6 eV are assigned to the Ni^{3+} chemical state.

Meanwhile, another peak at 880.5 eV and 862.3 eV accorded to the Ni^{2+} chemical state. The chemical states of $Co^{2+}/Co^{3+}/Co^{4+}$ and Ni^{2+}/Ni^{3+} in the sample are prone to support redox reactions and give benefits to enhancing the specific capacitance of supercapacitors. Additionally, the deconvoluted spectrum of O1 s in Figure 2f displayed the primary peak that can be divided into three fitting peaks at binding energy 534.5, 533.1, and 531.3 eV, which attributed to three oxygen species (referred to as O1, O2, and O3)(Dai et al., 2015; Li, Jiang, Zhou, Liu, & Zeng, 2015; J. Zhao, Li, Zhang, Meng, & Li, 2016). The O1 peak at high-level binding energy of

534.5 eV is ascribed to the typical metal-oxygen bonds. Meanwhile, the O3 peak at low binding energy 531.3 eV is attributed to the adsorbed water (hydroxyl groups) contained on the surface. The O2 appears at mid-level binding energy 533.1 due to low oxygen defects. All sample survey scans have confirmed the as-synthesized $CuCo_2O_4$-$Ni(OH)_2$ NWAs.

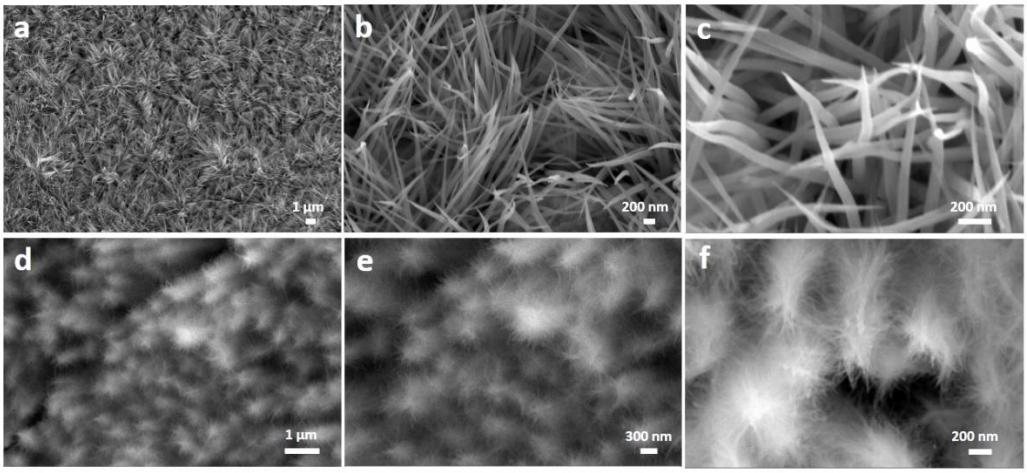

Figure 3. Representative SEM images with different magnifications of (a-c) $CuCo_2O_4$ nanowire and (d-f) hierarchical $CuCo_2O_4$-$Ni(OH)_2$ core-shell NWAs on Ni foam.

The morphological structures of $CuCo_2O_4$ nanowire and $CuCo_2O_4$-$Ni(OH)_2$ core-shell nanowire arrays (NWAs) were investigated by Scanning Electron Microscopy (SEM) with low and high magnifications. Figure 3a-c reveals the high-density grass-like $CuCo_2O_4$ nanowires deposited onto the entire Ni foam substrate. The magnified image shows the $CuCo_2O_4$ nanowire within the uniform length of ~300 nm, accompanied by shrinkage from the length of ~45 nm on the bottom to ~15 nm on the top of nanowire arrays. Meanwhile, the fascinated structures are depicted in Figure 3d-f, which reveals the homogenous shells of $Ni(OH)_2$ films within the length of ~70 nm to $CuCo_2O_4$ core and further to form $CuCo_2O_4$-$Ni(OH)_2$ core-shell nanowire arrays (NWAs). It is noticeable that a unique core-shell structure can influence enlarging electron pathways, shorting ion diffusion, and improving surface/interface interaction between electrode and electrolyte.

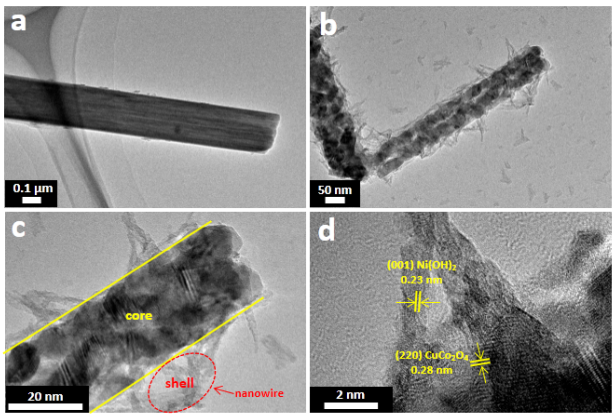

Figure 4. (a) TEM image of $CuCo_2O_4$ nanowire; (b-c) Low and high magnification TEM images of the hierarchical $CuCo_2O_4$-$Ni(OH)_2$ core-shell NWAs; (d) HRTEM image of the as-prepared $CuCo_2O_4$-$Ni(OH)_2$ core-shell NWAs.

More details of the microstructure of the as-prepared $CuCo_2O_4$ NW and $CuCo_2O_4$-$Ni(OH)_2$ NWAs are investigated by TEM and HRTEM analysis. As shown in Figure 4a, the prevalent $CuCo_2O_4$ with 1D nanowire arrays are grown vertically on the Ni foam surface. Figure 4b-c shows the notable alteration that has happened

to develop core-shell nanostructures of CuCo2O4-Ni(OH)2 NWAs consisting of small mesopore structures. The initial $CuCo_2O_4$ has been perpendicularly fledged by ultrathin $Ni(OH)_2$ nanowire arrays. The size of $CuCo_2O_4$-$Ni(OH)_2$ NWAs estimated in several nanometers further boosts active interfacial sites and facilitates faster electron transport pathways to introduce more significant pseudocapacitance properties. The HRTEM result is displayed in Figure 4e, with polycrystalline structure, and the core-shell of $CuCo_2O_4$-$Ni(OH)_2$ NWAs is investigated. The lattice fringes show the d-size of about 0.28 nm and 0.23, which are well-attributed to (220) and (001) planes of cubic $CuCo_2O_4$ and hexagonal $Ni(OH)_2$, respectively.

To measure the specific surface area and pore size distribution of materials, powder samples were characterized by nitrogen adsorption-desorption isotherm at 77 K. To determine the specific surface area, Brunauer-Emmet-Teller (BET) method was calculated for both materials.

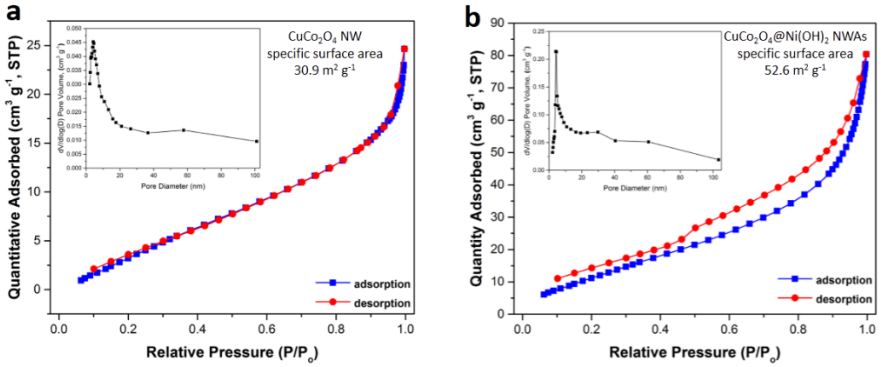

Figure 5. N_2 adsorption-desorption isotherms and pore size distribution curves (insets) for (a) $CuCo_2O_4$ nanowire and (b) $CuCo_2O_4$-$Ni(OH)_2$ core-shell NWAs.

Figure 5b shows that CuCo2O4-Ni(OH)2 NWAs have a specific surface area of 52.6 m2 g^{-1}, which is higher than $CuCo_2O_4$ (~30.9 m^2 g^{-1}) in Figure 5a. The corresponding pores size distribution was measured by Barrett-Joyner-Halenda (BJH) calculation. The pore size distribution of $CuCo_2O_4$ and $CuCo_2O_4$-$Ni(OH)_2$ NWAs is 5.63 nm and 7.53 nm, respectively, which indicates both as-prepared samples are mesoporous materials. All the as-reported properties have significantly increased $CuCo_2O_4$-$Ni(OH)_2$ NWAs characteristics. They are very desirable for supercapacitors application, specifically to the capability of faster ion transfer and contact between material and electrolyte.

Discussion

Electrochemical Properties

The main objective of this research is to investigate the materials as an appropriate electrodes in supercapacitors application. Hence, further analysis is required to determine the electrochemical properties of $CuCo_2O_4$ and $CuCo_2O_4$-$Ni(OH)_2$.

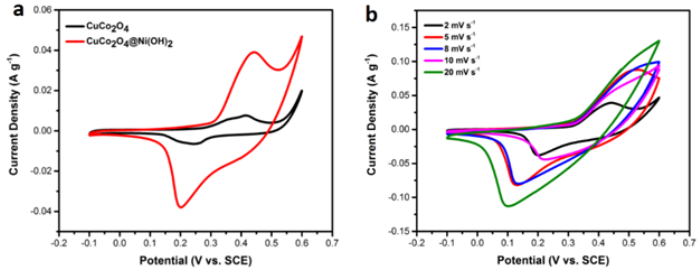

Figure 6. (a) CV comparison curves of $CuCo_2O_4$ NW and $CuCo_2O_4$-$Ni(OH)_2$ NWAs obtained at scan rates 2 mV s^{-1}; (b) CV curves of $CuCo_2O_4$-$Ni(OH)_2$ NWAs obtained at different scan rates.

All electrochemical performance evaluations were carried out in a three-electrode system. Both materials' cyclic voltammetry (CV) test was performed within the potential range of -0.1 to 0.6 V at different scan rates,

displayed in Figures 6a-b. The compared CV curves of $CuCo_2O_4$ NW and the hierarchical $CuCo_2O_4$-$Ni(OH)_2$ NWAs at 2 mV s^{-1} are shown in Figure 6a. From all curves, the perceptible redox peaks could be noticed, which indicates the occurrence of faradaic reactions. However, the $CuCo_2O_4$-$Ni(OH)_2$ NWAs significantly magnify the curve area rather than $CuCo_2O_4$, which is ascribed to the higher electrochemical activity on its hybrid core-shell nanowires structures. It also indicates that the electrode has larger capacitance and good surface area, which is credited to the build-up of $Ni(OH)_2$ onto the core material(K. Zhang et al., 2015). Figure 6b depicts the CV curves of CuCo2O4-Ni(OH)2 NWAs in different scan rates to observe more details. The redox peaks are still founded, marking the material has the essence of pseudocapacitive behavior.

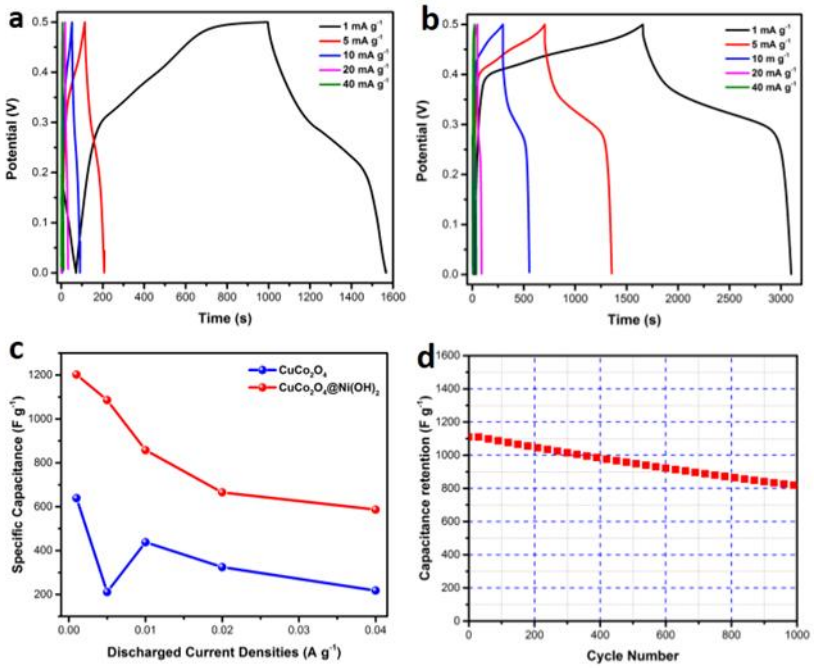

Figure 7. (a-b) Galvanostatic charge-discharge curves of $CuCo_2O_4$ NW and $CuCo_2O_4$-$Ni(OH)_2$ NWAs at different current densities; (c) Specific capacitances of $CuCo_2O_4$ NW (red curve) and $CuCo_2O_4$-$Ni(OH)_2$ NWAs (blue curve) calculated at various current densities; (d) the cycling performance of $CuCo_2O_4$-$Ni(OH)_2$ NWAs electrode.

Galvanostatic charge-discharge (GCD) evaluation was tested within voltage window range of 0 to 0.5 V in various current densities (1, 5, 10, 20, 40 mA g^{-1}). Figure 7a-b displays the charge-discharge curves of $CuCo_2O_4$ NW and $CuCo_2O_4$-$Ni(OH)_2$ NWAs, which both of them show distinct triangular symmetry areas resembling CV curves and denote the pseudocapacitive properties. The linear slopes transpired at low current densities of 1 to 10 mA g^{-1} for $CuCo_2O_4$ NW, indirectly estimating the morphology of a single CuCo2O4 nanowire impacts the reaction mechanism during the charge-discharge process. It also can be seen that the $CuCo_2O_4$-$Ni(OH)_2$ NWAs have a longer timespan than $CuCo_2O_4$ NW, which is attributed to high active electro ion adsorption-desorption within the electrode/electrolyte interface during the charge-discharge process. Subsequently, the charge-discharge curve of $CuCo_2O_4$-$Ni(OH)_2$ NWAs observed in near symmetry afford high coulombic efficiency and lower polarization within the electrode components. The specific capacitance was calculated from the slope of the discharged curve by using Equation (1). Figure 7c displays the specific capacitance of each electrode at different current densities.

The compared curve shows that the $CuCo_2O_4$-$Ni(OH)_2$ NWAs possess the uppermost specific capacitance of 1201.67 A g^{-1} at a current density of 1 mA g^{-1}, which altered to 586.67 A g^{-1} at the higher current density of 40 mA g^{-1}. Meanwhile, the $CuCo_2O_4$ NW delivers 638.89 A g^{-1} at a current density of 1 mA g^{-1} and drops to 217.78 A g^{-1} at 40 mA g^{-1}. The different curves also give the noticeable fact that the CuCo2O4-Ni(OH)2 NWAs have much more stability to retain the capacitance with different applied current densities. Remarkably, this specific capacitance is significantly higher than those of reported $CuCo_2O_4$-based material for supercapacitors,

such as CuCo2O4 maguey-like nanowires (982 F g^{-1} at 1.5 A g^{-1})(Liao et al., 2017), core-shell $CuCo_2O_4$@MnO_2 hetero-structured nanowire arrays on carbon fabrics (714 mF cm^{-2} at 1 mA cm^{-2})(Wang et al., 2014), and hierarchical $CuCo_2O_4$@$CuCo_2O_4$ nanowire arrays (888.9 F g^{-1} at 2 mA cm^{-2})(Y. Zhang et al., 2017).

Furthermore, cycling performance is another crucial factor to anticipate in the practical modes of supercapacitors. As depicted in Figure 7d, the capacitance at 5 mA g^{-1} alleviated in a minuscule number after 1000 cycles. It strongly keeps almost 84% capacitance retention from the initial capacitance, inherited by the good electrochemical stability on the electrode. This stunning cycling performance and another electrochemical property might be attributed to the following virtues of $CuCo_2O_4$-$Ni(OH)_2$ nanowire arrays electrode: (i) the core-shell nanostructure of $CuCo_2O_4$-$Ni(OH)_2$ NWAs possess high surface area, consequently provides much more electroactive sites for boosting electrochemical reactions41; (ii) the usage of Ni foam as a binder-free electrode and directly grown by $CuCo_2O_4$-$Ni(OH)_2$ NWAs, rendering open network pathways of electrolyte/electrode contact, henceforth paving more ion diffusion to the electrode(L. Zhang et al., 2013); (iii) the in-situ growth of $CuCo_2O_4$-$Ni(OH)_2$ NWAs on Ni foam by the hydrothermal method have enticed indomitable mechanical adhesion which fosters good electrical conductivity into the electrode(L. Zhang et al., 2016).

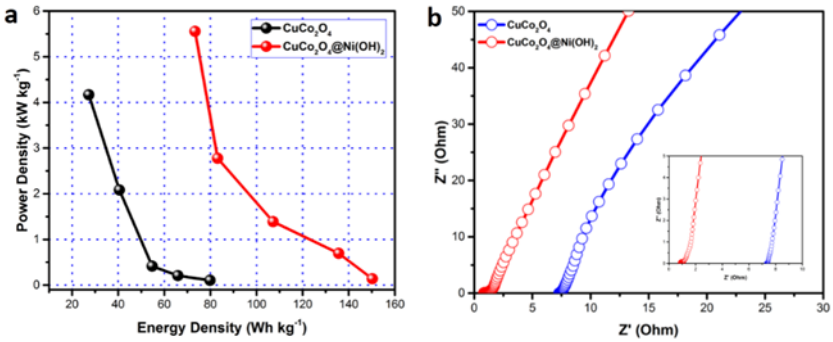

Figure 8. (a) The calculated Ragone plot of prepared electrodes; (b) The Nyquist plots of the EIS test with the frequency range of 0.01 Hz o 100 kHz. The magnified high-frequency region (inset).

The Ragone plots of $CuCo_2O_4$-$Ni(OH)_2$ NWAs and $CuCo_2O_4$ NW electrodes are displayed in Figure 8a. At a 73.33 Wh kg-1, the CuCo2O4-Ni(OH)2 NWAs present a much greater power density of 5.56 kW kg^{-1} than the $CuCo_2O_4$ NW electrode (power density 4.16 kW kg^{-1} at an energy density of 27.22 Wh kg^{-1}). Surprisingly, even at a higher energy density of 107.21 Wh kg-1, the CuCo2O4-Ni(OH)2 NWAs capable of detaining a power density of 1.38 kW kg^{-1}. The higher power density of $CuCo_2O_4$-$Ni(OH)_2$ NWAs is owing to the multitudinous oxidation states of redox reactions in the electrodes(Yin et al., 2015).

EIS study is another critical parameter for investigating electrochemical processes of supercapacitors electrodes. As shown in Figure 8b, the x-axis of the magnified high-frequency region symbolizes the equivalent series resistance (ESR), which involves three main resistances to the ionic electrolyte, the electrodes' active material, and the electrode interface and electrolyte. Seemingly, the $CuCo_2O_4$-$Ni(OH)_2$ NWAs (~1.09 Ω) present the lowest ESR, revealing that the core-shell NWAs have better electrical conductivity. The Nyquist plot of $CuCo_2O_4$-$Ni(OH)_2$ NWAs also shows the tiniest semicircle shape, which evident more active ion movement and lower charge transfer resistance than $CuCo_2O_4$ NW. Moreover, in the low-frequency range, the slope of the $CuCo_2O_4$-$Ni(OH)_2$ NWAs curve visibly shows more vertical lines, thus confirming better capacitive features followed by lower diffusion resistance(Hong et al., 2014). EIS study has again consistently demonstrated that $CuCo_2O_4$-$Ni(OH)_2$ NWAs own the highest electrochemical properties.

Conclusion

We have successfully fabricated CuCo2O4-Ni(OH)2 core-shell nanowire arrays via facile and cost-effective two-step hydrothermal process. The obtained $CuCo_2O_4$-$Ni(OH)_2$, incorporated by unique core-shell nanowire arrays, has capably attained great synergistic effects and significantly enhanced capacitance of 1201.67 F g^{-1} at 1 mA g^{-1} and remarkable power density of 5.56 kW kg^{-1} at energy density 73.33 Wh kg^{-1}. Astonishingly, at a higher energy density of 107.21 Wh kg-1, it is still capable of retaining a power density of 1.38 kW kg^{-1},

accompanied by good long-term cycling performance (~84 capacitance retention after 1000 cycles). From all the results, we believe a significant increment in electrochemical properties shows that $CuCo_2O_4$-$Ni(OH)_2$ core-shell nanowire arrays are very desirable for battery-type supercapacitors.

Acknowledgment

This work was supported by Fundamental Research Funds of the Central University (HEUCFZ), Heilongjiang Province Natural Science Funds for Distinguished Young Scholar (JC201404), Natural Science Foundation of Heilongjiang Province (B2015021), International Science & Technology Cooperation Program of China (2015DFR50050), the Major ijProject of Science and Technology of Heilongjiang Province (GA14A101), and Bandung State of Polytechnic.

References

Anu Prathap, M.U. Wei, C. Sun, S. and Xu, Z.J. 2015. A new insight into electrochemical detection of eugenol by hierarchical sheaf-like mesoporous NiCo2O4. Nano Research, 8(8): 2636-2645. doi:10.1007/s12274-015-0769-z

Chen, H. Hu, L. Yan, Y. Che, R. Chen, M. and Wu, L. 2013. One-Step Fabrication of Ultrathin Porous Nickel Hydroxide-Manganese Dioxide Hybrid Nanosheets for Supercapacitor Electrodes with Excellent Capacitive Performance. Advanced Energy Materials, 3(12): 1636-1646. doi:10.1002/aenm.201300580

Cheng, J. Yan, H. Lu, Y. Qiu, K. Hou, X. Xu, J. Han, L. Liu, X. Kim, J.-K. and Luo, Y. 2015. Mesoporous CuCo2O4nanograsses as multi-functional electrodes for supercapacitors and electro-catalysts. J. Mater. Chem. A, 3(18): 9769-9776. doi:10.1039/c5ta00408j

Chuo, H.X. Gao, H. Yang, Q. Zhang, N. Bu, W.B. and Zhang, X.T. 2014. Rationally designed hierarchical ZnCo2O4/Ni(OH)2nanostructures for high-performance pseudocapacitor electrodes. J. Mater. Chem. A, 2(48): 20462-20469. doi:10.1039/c4ta05319b

Cui, L. Huang, L. Ji, M. Wang, Y. Shi, H. Zuo, Y. and Kang, S. 2016. High-performance MgCo2O4 nanocone arrays grown on three-dimensional nickel foams: Preparation and application as binder-free electrode for pseudo-supercapacitor. Journal of Power Sources, 333: 118-124. doi:10.1016/j.jpowsour.2016.09.159

Dai, X. Chen, D. Fan, H. Zhong, Y. Chang, L. Shao, H. Wang, J. Zhang, J. and Cao, C.-n. 2015. Ni(OH) 2 /NiO/Ni composite nanotube arrays for high-performance supercapacitors. Electrochimica Acta, 154: 128-135. doi:10.1016/j.electacta.2014.12.066

Dyatkin, B. Presser, V. Heon, M. Lukatskaya, M.R. Beidaghi, M. and Gogotsi, Y. 2013. Development of a green supercapacitor composed entirely of environmentally friendly materials. ChemSusChem, 6(12): 2269-2280. doi:10.1002/cssc.201300852

Hong, W. Wang, J. Gong, P. Sun, J. Niu, L. Yang, Z. Wang, Z. and Yang, S. 2014. Rational construction of three dimensional hybrid Co 3 O 4 @NiMoO 4 nanosheets array for energy storage application. Journal of Power Sources, 270: 516-525. doi:10.1016/j.jpowsour.2014.07.149

Hu, J. Li, M. Lv, F. Yang, M. Tao, P. Tang, Y. Liu, H. and Lu, Z. 2015. Heterogeneous NiCo 2 O 4 @polypyrrole core/sheath nanowire arrays on Ni foam for high performance supercapacitors. Journal of Power Sources, 294: 120-127. doi:10.1016/j.jpowsour.2015.06.049

Khalid, S. Cao, C. Ahmad, A. Wang, L. Tanveer, M. Aslam, I. Tahir, M. Idrees, F. and Zhu, Y. 2015. Microwave assisted synthesis of mesoporous NiCo2O4 nanosheets as electrode material for advanced flexible supercapacitors. RSC Adv., 5(42): 33146-33154. doi:10.1039/c5ra02180d

Kurra, N. Alhebshi, N.A. and Alshareef, H.N. 2015. Microfabricated Pseudocapacitors Using Ni(OH)2Electrodes Exhibit Remarkable Volumetric Capacitance and Energy Density. Advanced Energy Materials, 5(2): 1401303. doi:10.1002/aenm.201401303

Li, W. Xin, L. Xu, X. Liu, Q. Zhang, M. Ding, S. Zhao, M. and Lou, X. 2015. Facile synthesis of three-dimensional structured carbon fiber-NiCo2O4-Ni(OH)2 high-performance electrode for pseudocapacitors. Scientific Reports, 5: 9277. doi:10.1038/srep09277

Li, X. Jiang, L. Zhou, C. Liu, J. and Zeng, H. 2015. Integrating large specific surface area and high conductivity in hydrogenated NiCo2O4 double-shell hollow spheres to improve supercapacitors. NPG Asia Materials, 7(3): e165. doi:10.1038/am.2015.11

Liao, L. Zhang, H. Li, W. Huang, X. Xiao, Z. Xu, K. Yang, J. Zou, R. and Hu, J. 2017. Facile synthesis of maguey-like CuCo 2 O 4 nanowires with high areal capacitance for supercapacitors. Journal of Alloys and Compounds, 695: 3503-3510. doi:10.1016/j.jallcom.2016.12.004

Liu, S. Hui, K.S. and Hui, K.N. 2016. Flower-like Copper Cobaltite Nanosheets on Graphite Paper as High-Performance Supercapacitor Electrodes and Enzymeless Glucose Sensors. ACS Appl Mater Interfaces, 8(5): 3258-3267. doi:10.1021/acsami.5b11001

Liu, S. San Hui, K. Hui, K.N. Yun, J.M. and Kim, K.H. 2016. Vertically stacked bilayer CuCo2O4/MnCo2O4 heterostructures on functionalized graphite paper for high-performance electrochemical capacitors. Journal of Materials Chemistry A, 4(21): 8061-8071. doi:10.1039/c6ta00960c

Lokhande, C.D. Dubal, D.P. and Joo, O.-S. 2011. Metal oxide thin film based supercapacitors. Current Applied Physics, 11(3): 255-270. doi:10.1016/j.cap.2010.12.001

Lokhande, V.C. Lokhande, A.C. Lokhande, C.D. Kim, J.H. and Ji, T. 2016. Supercapacitive composite metal oxide electrodes formed with carbon, metal oxides and conducting polymers. Journal of Alloys and Compounds, 682: 381-403. doi:10.1016/j.jallcom.2016.04.242

Pan, Y. Gao, H. Zhang, M. Li, L. Wang, G. and Shan, X. 2017. Three-dimensional porous ZnCo(2)O(4) sheet array coated with Ni(OH)(2) for high-performance asymmetric supercapacitor. Journal of Colloid and Interface Science, 497: 50-56. doi:10.1016/j.jcis.2017.02.053

Pendashteh, A. Moosavifard, S.E. Rahmanifar, M.S. Wang, Y. El-Kady, M.F. Kaner, R.B. and Mousavi, M.F. 2015. Highly Ordered Mesoporous CuCo2O4Nanowires, a Promising Solution for High-Performance Supercapacitors. Chemistry of Materials, 27(11): 3919-3926. doi:10.1021/acs.chemmater.5b00706

Wang , Q. Xu, J. Wang, X. Liu, B. Hou, X. Yu, G. Wang, P. Chen, D. and Shen, G. 2014. Core-Shell CuCo2O4@MnO2Nanowires on Carbon Fabrics as High-Performance Materials for Flexible, All-Solid-State, Electrochemical Capacitors. ChemElectroChem, 1(3): 559-564. doi:10.1002/celc.201300084

Wu, Z.-S. Zhou, G. Yin, L.-C. Ren, W. Li, F. and Cheng, H.-M. 2012. Graphene/metal oxide composite electrode materials for energy storage. Nano Energy, 1(1): 107-131. doi:10.1016/j.nanoen.2011.11.001

Xu, Y. Wang, X. An, C. Wang, Y. Jiao, L. and Yuan, H. 2014. Facile synthesis route of porous MnCo2O4and CoMn2O4nanowires and their excellent electrochemical properties in supercapacitors. J. Mater. Chem. A, 2(39): 16480-16488. doi:10.1039/c4ta03123g

Yin, Z. Zhang, S. Chen, Y. Gao, P. Zhu, C. Yang, P. and Qi, L. 2015. Hierarchical nanosheet-based NiMoO4 nanotubes: synthesis and high supercapacitor performance. Journal of Materials Chemistry A, 3(2): 739-745. doi:10.1039/c4ta05468g

Yu, A. Chen, Z. Maric, R. Zhang, L. Zhang, J. and Yan, J. 2015. Electrochemical supercapacitors for energy storage and delivery: Advanced materials, technologies and applications. Applied Energy, 153: 1-2. doi:10.1016/j.apenergy.2015.05.054

Zhang, K. Zeng, W. Zhang, G. Hou, S. Wang, F. Wang, T. and Duan, H. 2015. Hierarchical CuCo2O4 nanowire@NiCo2O4 nanosheet core/shell arrays for high-performance supercapacitors. RSC Advances, 5(85): 69636-69641. doi:10.1039/c5ra11007f

Zhang, L. Hui, K.N. Hui, K.S. Chen, X. Chen, R. and Lee, H. 2016. Role of graphene on hierarchical flower-like NiAl layered double hydroxide-nickel foam-graphene as binder-free electrode for high-rate hybrid supercapacitor. International Journal of Hydrogen Energy, 41(22): 9443-9453. doi:10.1016/j.ijhydene.2016.04.050

Zhang, L. Wang, J. Zhu, J. Zhang, X. San Hui, K. and Hui, K.N. 2013. 3D porous layered double hydroxides grown on graphene as advanced electrochemical pseudocapacitor materials. Journal of Materials Chemistry A, 1(32): 9046. doi:10.1039/c3ta11755c

Zhang, Y. Xu, J. Zheng, Y. Zhang, Y. Hu, X. and Xu, T. 2017. Construction of CuCo2O4@CuCo2O4 hierarchical nanowire arrays grown on Ni foam for high-performance supercapacitors. RSC Advances, 7(7): 3983-3991. doi:10.1039/c6ra25970g

Zhao, J. Li, Z. Zhang, M. Meng, A. and Li, Q. 2016. Direct Growth of Ultrathin NiCo2O4/NiO Nanosheets on SiC Nanowires as a Free-Standing Advanced Electrode for High-Performance Asymmetric Supercapacitors. ACS Sustainable Chemistry & Engineering, 4(7): 3598-3608. doi:10.1021/acssuschemeng.6b00697

Zhao, Y. Hu, L. Zhao, S. and Wu, L. 2016. Preparation of MnCo2O4@Ni(OH)2Core-Shell Flowers for Asymmetric Supercapacitor Materials with Ultrahigh Specific Capacitance. Advanced Functional Materials, 26(23): 4085-4093. doi:10.1002/adfm.201600494